

Synthesis and Characterization of Divalent Lanthanide Selenolates and Tellurolates. X-ray Crystal Structures of $\text{Yb}[\text{SeSi}(\text{SiMe}_3)_3]_2(\text{TMEDA})_2$ and $\{\text{Eu}[\text{TeSi}(\text{SiMe}_3)_3]_2(\text{DMPE})_2\}_2(\mu\text{-DMPE})$

Douglas R. Cary and John Arnold*

Department of Chemistry, University of California, Berkeley, California 94720

Received November 4, 1993*

A series of divalent lanthanide chalcogenolates of empirical formula $\text{Ln}[\text{ESi}(\text{SiMe}_3)_3]_2(\text{TMEDA})_2$ ($\text{Ln} = \text{Yb}, \text{Eu}, \text{Sm}$; $\text{E} = \text{Se}, \text{Te}$; $\text{TMEDA} = \text{Me}_2\text{NCH}_2\text{CH}_2\text{NMe}_2$) and $\{\text{Eu}[\text{ESi}(\text{SiMe}_3)_3]_2(\text{DMPE})_2\}_2(\mu\text{-DMPE})$ ($\text{E} = \text{Se}, \text{Te}$; $\text{DMPE} = \text{Me}_2\text{PCH}_2\text{CH}_2\text{PMe}_2$) have been prepared by the reaction of $\text{Ln}[\text{N}(\text{SiMe}_3)_2]_2(\text{THF})_2$ ($\text{Ln} = \text{Yb}, \text{Eu}, \text{Sm}$) with $\text{HESi}(\text{SiMe}_3)_3$ ($\text{E} = \text{Se}, \text{Te}$) in diethyl ether with excess TMEDA or DMPE. Both $\text{Yb}[\text{SeSi}(\text{SiMe}_3)_3]_2(\text{TMEDA})_2$ and $\{\text{Eu}[\text{ESi}(\text{SiMe}_3)_3]_2(\text{DMPE})_2\}_2(\mu\text{-DMPE})$ have been structurally characterized by X-ray crystallography. $\text{Yb}[\text{SeSi}(\text{SiMe}_3)_3]_2(\text{TMEDA})_2$ crystallizes at -40°C from hexanes in the space group $P2_1/c$ with $a = 9.441(2)\text{ \AA}$, $b = 12.311(2)\text{ \AA}$, $c = 23.407(7)\text{ \AA}$, $\beta = 96.013(21)^\circ$, $V = 2705.4(11)\text{ \AA}^3$, $d_{\text{calcd}} = 1.30\text{ g cm}^{-3}$, and $Z = 2$. $\{\text{Eu}[\text{ESi}(\text{SiMe}_3)_3]_2(\text{DMPE})_2\}_2(\mu\text{-DMPE})$ crystallizes at -40°C from hexanes in the space group $P\bar{1}$ with $a = 13.629(2)\text{ \AA}$, $b = 13.696(2)\text{ \AA}$, $c = 17.642(3)\text{ \AA}$, $\alpha = 81.715(13)^\circ$, $\beta = 78.828(12)^\circ$, $\gamma = 89.452(13)^\circ$, $V = 3190.2(12)\text{ \AA}^3$, $d_{\text{calcd}} = 1.33\text{ g cm}^{-3}$, and $Z = 2$. On being heated to ca. 200°C in the solid state, the Yb–TMEDA compounds eliminate $\text{E}[\text{Si}(\text{SiMe}_3)_3]_2$ to form the corresponding divalent chalcogenides as dark, microcrystalline powders.

Introduction

It has been known for many years that chemistry of chalcogenolate complexes is dominated by the formation of oligomeric or polymeric structures resulting from bridging interactions via lone pairs on the chalcogen.^{1,2} Development of the molecular chemistry of these compounds has been slow, since they are frequently insoluble in common organic solvents and are, therefore, difficult to purify and characterize.¹ Aryl chalcogenolate ligands with bulky ortho substituents have been useful in the isolation of low-molecularity species, particularly for the lighter chalcogens,^{3–5} but polymeric products may still be formed with the heavier group 16 element analogs, selenolates and tellurolates, especially if the ortho substituent is not large enough to effectively hinder the chalcogen.^{6,7}

Much of the recent interest in lanthanide chalcogenolates results from their possible use as precursors to lanthanide chalcogenides.^{8–10} These materials are of wide interest due to their unusual magnetic, electronic, and optical properties.¹¹ Lanthanide chalcogenolates have also been prepared in redox reactions aimed at probing the chemistry of ytterbium(II) and samarium(II) complexes.^{12–15} In addition, two further motivations to study

these compounds are (i) that the combination of a hard, electropositive metal and a soft, polarizable ligand may result in reactive metal–ligand bonds and (ii) that relatively few examples of these types of materials are known.^{9,16}

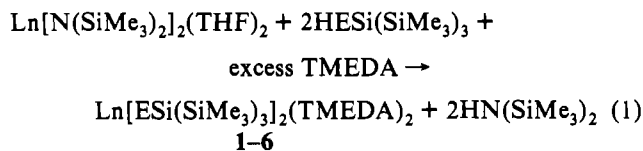
Our recent work in metal chalcogenolate chemistry has resulted in the development of a new series of sterically demanding tellurolate, selenolate, and thiolate ligands based on the bulky silyl substituent $-\text{Si}(\text{SiMe}_3)_3$.^{17,18} The utility of these ligands in forming stable, well-defined complexes of low molecularity and increased hydrocarbon solubility has now been demonstrated for a wide range of main-group and transition metal systems.^{9,19–26} Here we describe the synthesis and characterization of some divalent lanthanide complexes and preliminary results indicating their potential as precursors to lanthanide chalcogenides.

Results and Discussion

TMEDA Derivatives. The protonolysis reaction between $\text{Ln}[\text{N}(\text{SiMe}_3)_2]_2(\text{THF})_2$ ($\text{Ln} = \text{Yb}, \text{Eu}, \text{Sm}$) and $\text{HESi}(\text{SiMe}_3)_3$ ($\text{E} = \text{Se}, \text{Te}$) in the presence of TMEDA in hydrocarbon solvents or diethyl ether provides a simple method of preparing monomeric divalent lanthanide chalcogenolates (eq 1). Monitoring of the Yb and Sm reactions by ^1H NMR spectroscopy indicated quantitative conversion to products. On preparative scales, crystallization from hexanes allows 1–6 to be isolated in yields that typically range from 53 to 72%.

- * Abstract published in *Advance ACS Abstracts*, March 15, 1994.
- Gysling, H. J. In *The Chemistry of Organic Selenium and Tellurium Compounds*; Patai, S. Rappoport, Z., Ed.; Wiley: New York, 1986; Vol. 1, Chapter 18.
 - Dance, I. G. *Polyhedron* 1986, 5, 1037.
 - Mehrotra, R. C.; Singh, A.; Tripathi, U. M. *Chem. Rev.* 1991, 91, 1287.
 - Bochmann, M.; Webb, K.; Harman, M.; Hursthouse, M. B. *Angew. Chem., Int. Ed. Engl.* 1990, 29, 638.
 - Cetinkaya, B.; Hitchcock, P. B.; Lappert, M. F.; Smith, R. G. *J. Chem. Soc., Chem. Commun.* 1992, 932.
 - Bochmann, M.; Coleman, A. P.; Webb, K. J.; Hursthouse, M. B.; Mazid, M. *Angew. Chem., Int. Ed. Engl.* 1991, 30, 973.
 - Bochmann, M.; Webb, K. J. *J. Chem. Soc., Dalton Trans* 1991, 2325.
 - Strzelecki, A. R.; Timinski, P. A.; Helsen, B. A.; Bianconi, P. A. *J. Am. Chem. Soc.* 1992, 114, 3159.
 - Cary, D. R.; Arnold, J. J. *Am. Chem. Soc.* 1993, 115, 2520.
 - Berardini, M.; Emge, T.; Brennan, J. G. *J. Am. Chem. Soc.* 1993, 115, 8501.
 - Handbook of the Physics and Chemistry of Rare Earths*; Gschneidner, K. A., Eyring, L., Eds.; North-Holland: Amsterdam, 1978.
 - Berg, D. J.; Andersen, R. A.; Zalkin, A. *Organometallics* 1988, 7, 1858.
 - Berg, D. J.; Burns, C. J.; Andersen, R. A.; Zalkin, A. *Organometallics* 1989, 8, 1865.

- Recknagel, A.; Noltemeyer, M.; Stalke, D.; Pieper, U.; Schmidt, H.-G.; Edelmann, F. T. *J. Organomet. Chem.* 1991, 411, 347.
- Wedler, M.; Recknagel, A.; Gilje, J. W.; Noltemeyer, M.; Edelmann, F. T. *J. Organomet. Chem.* 1992, 426, 295.
- Schumann, H.; Albrecht, I.; Gallagher, M.; Hahn, E.; Janiak, C.; Kolax, C.; Loebel, J.; Nickel, S.; Palamidis, E. *Polyhedron* 1988, 7, 2307.
- Bonasia, P. J.; Gindelberger, D. E.; Dabbousi, B. O.; Arnold, J. J. *Am. Chem. Soc.* 1992, 114, 5209.
- Bonasia, P. J.; Christou, V.; Arnold, J. J. *Am. Chem. Soc.* 1993, 115, 6777.
- Bonasia, P. J.; Arnold, J. *Inorg. Chem.* 1992, 31, 2508.
- Gindelberger, D. E.; Arnold, J. J. *Am. Chem. Soc.* 1992, 114, 6242.
- Christou, V.; Arnold, J. J. *Am. Chem. Soc.* 1992, 114, 6240.
- Seligson, A. L.; Arnold, J. J. *Am. Chem. Soc.* 1993, 115, 8214.
- Gindelberger, D. E.; Arnold, J. *Inorg. Chem.* 1993, 32, 5813.
- Christou, V.; Wuller, S. P.; Arnold, J. J. *Am. Chem. Soc.* 1993, 115, 10545.
- Bonasia, P. J.; Mitchell, G. P.; Hollander, F. J.; Arnold, J. *Inorg. Chem.*, following paper in this issue.
- Christou, V.; Arnold, J. *Angew. Chem., Int. Ed. Engl.* 1993, 32, 1450.



E = Se; Ln = Yb (1), Eu (3), Sm (5)

E = Te; Ln = Yb (2), Eu (4), Sm (6)

The selenolates and tellurolates crystallize as highly-colored (Yb, orange; Eu, yellow; Sm, dark green) air- and moisture-sensitive thin needles or plates, respectively. Under an atmosphere of dry N_2 , significant decomposition (in solution or the solid state) occurs within about 12 h at room temperature under normal lighting conditions. Although not studied in detail, both heat and light appear to contribute separately to this decomposition. Storage of these compounds at -40°C in the dark prevents decomposition over the course of at least a couple weeks. Recrystallization from large volumes of hexanes gives analytically pure Yb and Eu compounds, while the Sm chalcogenolates retain minor SiMe_3 -containing decomposition products, even after repeated recrystallizations. Preparation of **5** or **6** by the metathesis reaction between $\text{SmI}_2(\text{THF})_2$ and $\text{KESi}(\text{SiMe}_3)_3$ (E = Se, Te) in the presence of TMEDA or the preparation of **6** by the reduction of $\text{Sm}[\text{N}(\text{SiMe}_3)_2]_3$ with 3 equiv of $\text{HTeSi}(\text{SiMe}_3)_3$ in the presence of TMEDA also shows the same mixture of decomposition products. In general, higher yields and ease of purification make the protonolysis route preferable to the salt-elimination route.¹⁹

The ^1H NMR spectrum of **2** shows three singlets: two for the TMEDA ligands at 2.44 and 2.22 ppm (relative ratio 24:8), and a single peak due to the two tellurolates at 0.46 ppm (relative ratio 54). Signals corresponding to the two ligands were detected in the $^{13}\text{C}\{^1\text{H}\}$ NMR spectrum at 56.6, 50.0, and 1.64 ppm. The tellurolate ligands also give rise to a singlet at 610 ppm in the $^{125}\text{Te}\{^1\text{H}\}$ NMR spectrum, in the range typical for early metal complexes of this ligand.^{9,21,24} Analogous ^1H and $^{13}\text{C}\{^1\text{H}\}$ spectra were obtained for **1**; however, we could not detect a ^{77}Se resonance, presumably due to the compound's low solubility in benzene- d_6 . Attempts to observe ^{171}Yb NMR signals for either compound were also unsuccessful.

The Eu(II) compounds **3** and **4** show only a very broad ^1H NMR resonance centered around 0 ppm. This feature is ascribed to the large magnetic moments involved, which fall in the range expected for the f^7 Eu(II) center²⁷ (**3**, $\mu_{\text{eff}} = 8.1 \mu_{\text{B}}$; **4**, $\mu_{\text{eff}} = 8.0 \mu_{\text{B}}$).

More informative ^1H NMR spectra were recorded for the Sm(II) derivatives, **5** and **6**, each of which showed three singlets in the ratio 8:54:24, indicating a structure analogous to those of **1** and **2** above. In the Sm(II) compounds, however, the peaks are shifted and broadened due to coupling from the paramagnetic metal centers [**5**, $\mu_{\text{eff}} = 3.4 \mu_{\text{B}}$, δ 5.96 ($\Delta\nu_{1/2} = 44$ Hz), 1.30 ($\Delta\nu_{1/2} = 4.5$ Hz), -20.05 ($\Delta\nu_{1/2} = 19$ Hz); **6**, $\mu_{\text{eff}} = 3.3 \mu_{\text{B}}$, δ 3.02 ($\Delta\nu_{1/2} = 62$ Hz), 1.97 ($\Delta\nu_{1/2} = 14$ Hz), -21.02 ($\Delta\nu_{1/2} = 93$ Hz)]. Plots of the ^1H chemical shifts vs. $1/T$ from 210 to 330 K are linear for both compounds, indicating simple Curie-Weiss behavior.^{28,29} Coupling to unpaired electrons also explains why only one resonance, presumably due to the chalcogenolate ligand, is observed in the $^{13}\text{C}\{^1\text{H}\}$ NMR spectrum of each compound (0.89

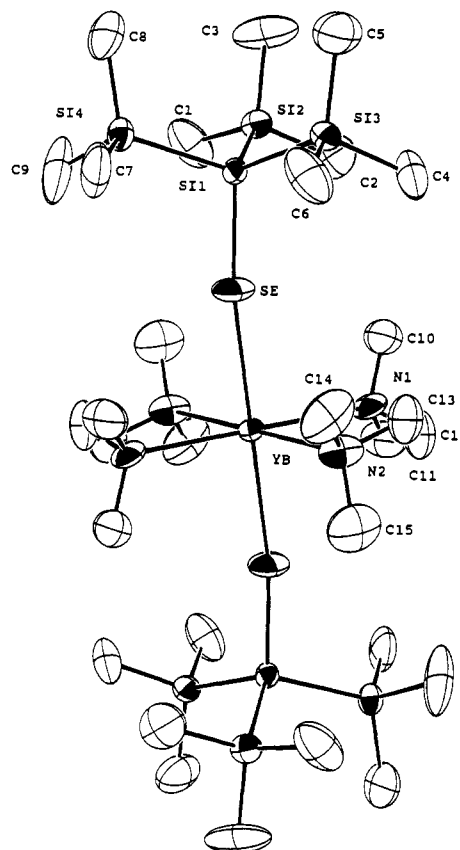


Figure 1. ORTEP view of $\text{Yb}[\text{SeSi}(\text{SiMe}_3)_3]_2(\text{TMEDA})_2$ (**1**). Thermal ellipsoids are drawn at the 50% probability level. Hydrogen atoms are omitted for clarity.

Table 1. Crystallographic Data Collection Parameters for **1** and **8**

	1	8
formula	$\text{C}_{30}\text{H}_{86}\text{N}_4\text{Si}_8\text{Se}_2\text{Yb}$	$\text{C}_{33}\text{H}_{94}\text{P}_5\text{Si}_8\text{Te}_2\text{Eu}$
mol weight	1058.7	1277.8
space group	$P2_1/c$	$P\bar{1}$
$a/\text{\AA}$	9.441(2)	13.629(2)
$b/\text{\AA}$	12.311(2)	13.696(2)
$c/\text{\AA}$	23.407(7)	17.642(3)
α/deg	90	81.715(13)
β/deg	96.013(21)	78.828(12)
γ/deg	90	89.452(13)
vol/ \AA^3	2705.4(11)	3190.2(12)
Z	2	2
$d_{\text{calcd}}/\text{g cm}^{-3}$	1.30	1.33
crystal size/mm	$0.15 \times 0.20 \times 0.20$	$0.19 \times 0.32 \times 0.46$
radiation ($\lambda/\text{\AA}$)	$\text{Mo K}\alpha$ (0.710 73)	$\text{Mo K}\alpha$ (0.710 73)
scan mode	$\theta-2\theta$	$\theta-2\theta$
2θ range/deg	3-45	3-50
colcn range	$\pm h, +k, +l$	$+h, \pm k, \pm l$
abs coeff, μ	32.4	21.7
no. of unique reflcns	3408	11125
no. of reflcns with $F^2 > 3\sigma(F^2)$	1986	8565
final R, R_w	0.0437, 0.0424	0.0350, 0.0410
$T/^\circ\text{C}$	-104	-90

ppm in **5** and 1.59 ppm in **6**). Despite its proximity to the paramagnetic Sm(II) center, the tellurolate ligand in **6** still gives rise to a measurable $^{125}\text{Te}\{^1\text{H}\}$ NMR spectrum, which shows a remarkably low-field singlet at 3243 ppm. Again, the ^{77}Se NMR spectrum of the selenolate derivative (**5**) could not be obtained due to solubility limitations.

X-ray Structure of 1. A view of the solid-state molecular structure of **1** is shown in Figure 1, with selected bond lengths and angles provided in Table 2. The six-coordinate Yb atom sits on a crystallographically imposed center of inversion. As expected based on differences in ionic radii between divalent and trivalent

(27) Cotton, S. *Lanthanides and Actinides*; Oxford University Press: New York, 1991, p 192.

(28) Jesson, V. P. in *NMR of Paramagnetic Molecules*; La Mar, G. N., Horrocks, W. D., Jr., Holm, R. H., Ed.; Academic Press: New York, 1973; Chapter 1.

(29) Linear behavior was not observed for the plot of the TMEDA methyl resonance of **6**. The peak broadened and disappeared below 254 K, presumably due to exchange of diastereotopic methyl groups slowing down at low temperature. Cooling to 210 K did not slow this exchange sufficiently for new peaks to appear, and further cooling was prevented by solubility limitations.

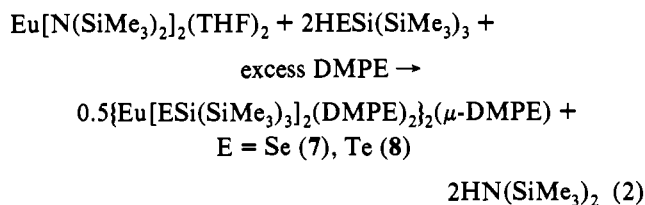
Table 2. Selected Bond Distances (Å) and Angles (deg) for **1**

Yb–Se	2.870(1)	Yb–N2	2.577(10)
Yb–N1	2.586(10)	Se–Si1	2.238(3)
Se–Yb–N1	93.39(23)	N1–Yb–N2	73.6(4)
Se–Yb–N1	86.61(23)	N1–Yb–N2	106.4(4)
Se–Yb–N2	88.26(22)	Yb–Se–Si1	163.71(11)
Se–Yb–N2	91.74(22)		

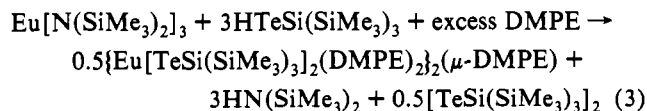
Yb (0.15 Å),³⁰ the Yb–Se bond length (2.870(1) Å) is slightly longer than those reported for related six-coordinate Yb(III) species [PhC(NSiMe₃)₂]₂Yb(SeAr)(THF) (Ar = Ph, Yb–Se = 2.805(1) Å;³¹ Ar = mesityl, Yb–Se = 2.793(2) Å).¹⁵ Calculations based on ionic radii are less accurate at predicting the absolute Yb–Se bond distance, with the predicted value of 3.00 Å being significantly longer than that observed experimentally.³⁰ The Yb–N bond lengths, 2.586(10) and 2.577(10) Å, are close to that reported for Cp*₂Yb(TePh)(NH₃) (Yb–N = 2.50(1) Å).¹²

Due to the inversion center, the Se–Yb–Se angle is required to be 180°. The Yb–Se–Si bond angle (163.71(11)°) is extremely large compared to those in [PhC(NSiMe₃)₂]₂Yb(SeAr)(THF) (Ar = Ph, Yb–Se–C = 105.3(3)°;³¹ Ar = mesityl, Yb–Se–C = 109.0(2)°)¹⁵ and Cp*₂Sm(Se-2,4,6-C₆H₂(CF₃)₃)(THF) (Sm–Se–C = 126.4(1)°).¹⁴ This unusual feature may be ascribed to increased interligand repulsion resulting from the greater steric bulk of the –SeSi(SiMe₃)₃ group. The angle between the least-squares plane containing Yb, Se, and Si1 and the plane containing Yb, N1, and N2 is 89.87(24)°. Simple electrostatic considerations predict the observed trans, pseudooctahedral geometry observed.³² Metrical parameters for the silyl groups and TMEDA ligands are not unusual, and there are no unusually close intermolecular contacts.

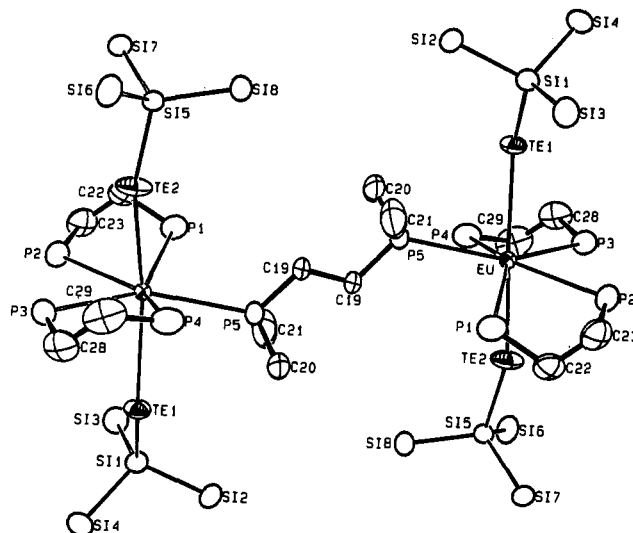
Europium DMPE Derivatives. In order to compare N versus P donor ligands on the chemistry of lanthanide(II) chalcogenolates, we attempted to prepare the DMPE analogs of **3** and **4** using similar reaction conditions. As shown in eq 2, however, the



products **7** and **8** are somewhat different, with coordination of a fifth donor atom resulting in the formation of seven-coordinate μ -DMPE dimers. The differing structures presumably arise as a consequence of the larger covalent radius of phosphorus relative to nitrogen, leading to longer Eu–P bonds and a less crowded metal center for a given coordination number. Removal of the volatiles and crystallization from hexanes gives pure **7** and **8** in 69 and 58% yields, respectively. Compound **8** was also formed in attempts to prepare a trivalent europium tellurolate, as shown in eq 3.



Reduction of Ln(III) to Ln(II) also occurs for Sm and Yb. These latter reactions are not surprising, as tellurolate anions are

**Figure 2.** ORTEP view of {Eu[TeSi(SiMe₃)₃]₂(DMPE)₂}(μ-DMPE) (**8**). Thermal ellipsoids are drawn at the 50% probability level. Hydrogen and selected carbon atoms are omitted for clarity.**Table 3.** Selected Bond Distances (Å) and Angles (deg) for **8**

Eu–Te1	3.234(1)	Eu–P3	3.168(1)
Eu–Te2	3.159(1)	Eu–P4	3.165(2)
Eu–P1	3.249(2)	Eu–P5	3.185(1)
Eu–P2	3.217(1)		
Te1–Eu–Te2	154.73(1)	Te2–Eu–P4	80.31(3)
Te1–Eu–P1	125.31(3)	Te2–Eu–P5	105.43(3)
Te1–Eu–P2	107.31(3)	P1–Eu–P2	64.83(4)
Te1–Eu–P3	78.54(3)	P2–Eu–P3	75.99(5)
Te1–Eu–P4	77.14(3)	P3–Eu–P4	67.30(5)
Te1–Eu–P5	81.09(3)	P4–Eu–P5	78.39(5)
Te2–Eu–P1	79.92(3)	P1–Eu–P5	78.24(5)
Te2–Eu–P2	83.67(3)	Eu–Te1–Si1	130.64(4)
Te2–Eu–P3	82.38(3)	Eu–Te2–Si5	164.45(4)

easily oxidized³³ and the reduction Ln(III) + e[−] → Ln(II) for Eu, Sm, and Yb is quite facile.²⁷ In contrast, the less-reducing selenolate ligand forms stable Ln(III) derivatives under comparable conditions.³⁴

The selenolate and tellurolate compounds crystallize as air- and moisture-sensitive thin needles or blocks, respectively. Under an atmosphere of dry N₂, they can be stored for several weeks under normal lighting conditions without decomposition. The room temperature magnetic moments of **7** and **8** ($\mu_{\text{eff}} = 8.0 \mu_{\text{B}}$ for both compounds) are high enough to prevent the use of NMR spectroscopy in their characterization. Variable-temperature solid-state magnetic susceptibility measurements for **8** indicate simple paramagnetic behavior down to 5 K ($\chi_{\text{m}} = C/(T - \theta)$, $C = 7.55$, $\theta = 1.23$ K).

X-ray Structure of 8. An ORTEP view of the molecular structure of **8** is shown in Figure 2, and Table 3 contains selected bond lengths and angles. Each Eu atom is seven-coordinate with the tellurolate ligands occupying axial positions. There is an inversion center between C19 and C19' of the bridging DMPE ligand, and an approximate mirror plane including the Eu atoms and bridging ligand. The five phosphorus atoms and europium atom are nearly coplanar. Direct comparison of the Eu–Te and Eu–P bond lengths to related compounds is hampered by the lack of any other published structures of europium tellurolates or phosphines.³⁵ There are no close inter- or intramolecular contacts in the molecule.

(33) Jensen, K. A.; Kjær, A. In *The Chemistry of Organic Selenium and Tellurium Compounds*; Patai, S., Rappoport, Z., Eds.; Wiley: New York, 1986; Vol. 1; p 6.

(34) Cary, D. R.; Arnold, J. Work in progress.

(35) Cambridge Structural Database. Address: Cambridge Crystallographic Data Centre, 12 Union Road, GB-Cambridge CB2 1EZ, England.

(30) Shannon, R. D. *Acta Crystallogr., Sect. A* 1976, A32, 751.

(31) Wedler, M.; Noltemeyer, M.; Pieper, U.; Schmidt, H.-G.; Stalke, D.; Edelmann, F. T. *Angew. Chem., Int. Ed. Engl.* 1990, 29, 894.

(32) Kepert, D. L. *Prog. Inorg. Chem.* 1977, 23, 1.

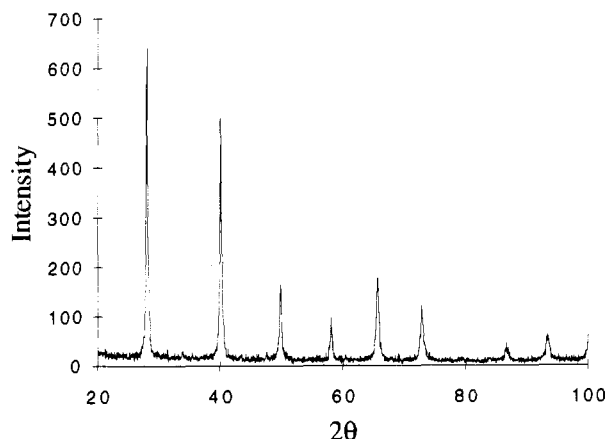
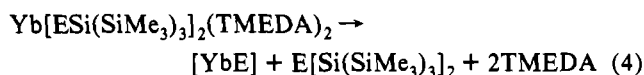


Figure 3. XRD spectrum of YbTe from the thermolysis of Yb[TeSi(SiMe₃)₃]₂(TMEDA)₂ (2).

As in the case of **1** above, calculations based on ionic radii predict M–E bond lengths that are significantly longer than those actually observed. In the present case, Eu–Te bond lengths are 3.234(1) and 3.159(1) Å, while the summation of ionic radii predicts 3.41 Å.³⁰ For comparison, in the solid-state compound EuTe the bond length is 3.29 Å.³⁶ The Eu–P bond lengths (average 3.20(1) Å) are roughly 0.2 Å longer than in Yb[N(SiMe₃)₂]₂(DMPE) (3.012(4) Å),³⁷ a result which merely reflects the difference in the ionic radii of Eu(II) and Yb(II) (ca. 0.30 Å larger for Eu(II)).³⁰ The phosphine bite angles in these two compounds are also quite similar (P–Eu–P average 66.1(1)° and P–Yb–P 68.4(2)°). In contrast to the six-coordinate selenolate **1** described above, the chalcogenolate ligands in seven-coordinate **8** are not linearly disposed about the metal (Te–Eu–Te = 154.73(1)°). It is also noteworthy that the angles at the chalcogen atoms are quite different, with one (Eu–Te₂–Si₅ = 164.34(4)°) being close to the related parameter in the selenolate **1** (Yb–Se–Si = 163.71(11)°) whereas the other is much more acute (Eu–Te₁–Si₁ = 130.64(4)°).

Solid-State Thermolyses. For the Yb–TMEDA compounds, preliminary results indicate that they can be converted to the corresponding divalent metal chalcogenides by heating to 150–200 °C in the solid state at 10^{–2} Torr (eq 4).



Decomposition of metal chalcogenolates in this manner is well documented, having been observed to occur in bulk solids, in solution, and in the gas phase.^{4,8,9,38–41}

In the present case, the formation of pure E[Si(SiMe₃)₃]₂ (E = Se, Te) was confirmed by ¹H and ¹³C{¹H} NMR spectroscopy. The black powders recovered after heating to 300 °C contained low levels of carbon (typically: C, <3%; H and N, 0.0%), but were not very crystalline, as determined by X-ray powder diffraction. Annealing at 800 °C lowered the carbon levels slightly, while significantly improving crystallinity. Figure 3 shows a typical XRD spectrum of YbTe obtained from the

thermolysis of **2**. The XRD spectra obtained for YbE (E = Se, Te) produced in each thermolysis match those of the known compounds. Full details of thermolysis and other reactions of compounds **1–8** will be reported later.³⁴

Experimental Section

General Data. Standard air- and moisture-sensitive techniques were used as previously described.¹⁷ The compounds Ln[N(SiMe₃)₂]₂(THF)₂ (Ln = Eu, Yb),^{42,43} Sm[N(SiMe₃)₂]₂(THF)₂,⁴⁴ SmI₂(THF)₂,⁴⁵ HESi(SiMe₃)₃ (E = Se, Te),¹⁸ KESi(SiMe₃)₃ (E = Se, Te),⁴⁶ and (H₃C)₂PCH₂CH₂P(CH₃)₂ (DMPE)⁴⁷ were prepared by literature methods. Melting points were determined in capillaries sealed under N₂ and are uncorrected. Samples for FT IR spectroscopy were prepared as Nujol mulls between KBr plates. Room temperature magnetic moments were determined by the Evans method.⁴⁸ Variable temperature magnetic susceptibilities were measured using a superconducting quantum interference device (SQUID). All magnetic susceptibilities are corrected for the underlying diamagnetic susceptibility.⁴⁹ Unless otherwise stated, all NMR spectra were recorded at 400 MHz for ¹H, 101 MHz for ¹³C, and 94.7 MHz for ¹²⁵Te at room temperature using C₆D₆ as the solvent. Chemical shifts for ¹H NMR spectra are relative to tetramethylsilane and were calibrated by measurement of the chemical shifts of the residual protons in the deuterated solvents used. Chemical shifts for ¹³C{¹H} NMR spectra are relative to tetramethylsilane and were calibrated by measurement of the chemical shifts of the deuterated solvents. Chemical shifts for ¹²⁵Te{¹H} NMR spectra are relative to Me₂Te and were calibrated with external Te(OH)₆ (δ 712 ppm). X-ray powder diffraction (XRD) patterns were recorded on ground samples stuck to a quartz slide with petroleum jelly using an automated Siemens diffractometer with Cu Kα radiation and standard data reduction software. Elemental analyses were performed at the microanalytical laboratory in the College of Chemistry, University of California, Berkeley, CA, and Desert Analytics, Tucson, AZ.

Yb[SeSi(SiMe₃)₃]₂(TMEDA)₂ (1). The addition of 40 mL of diethyl ether and 5 mL of TMEDA to a flask containing Yb[N(SiMe₃)₂]₂(THF)₂ (428 mg, 0.671 mmol) and HSeSi(SiMe₃)₃ (439 mg, 1.34 mmol) resulted in the immediate formation of a homogeneous yellow-orange solution. After 10 min of stirring, the volatiles were removed under vacuum. Extraction of the resulting solid with 150 mL of hexanes, followed by concentration and cooling to –40 °C, yielded thin yellow-orange needles of **1** (483 mg, 68%). Recrystallization from hexanes gave crystals suitable for X-ray diffraction. Anal. Calcd for C₃₀H₈₆N₄Si₈Se₂Yb: C, 34.04; H, 8.19; N, 5.29. Found: C, 34.20; H, 8.26; N, 5.29. Mp: 213–215 °C dec. ¹H NMR: δ 2.42 (s, 24 H), 2.27 (s, 8 H), 0.42 (s, 54 H). ¹³C{¹H} NMR: δ 56.8, 49.4, 1.15. IR (cm^{–1}): 1917 w, 1854 w, 1410 w, 1356 w, 1299 w, 1290 m, 1254 m, 1231 s, 1185 w, 1161, 1127 m, 1101 w, 1071 m, 1028 s, 1015 m, 953 s, 918 w, 866 s, 836 s, 784 s, 774 m, 740 m, 685 s, 624 s.

Yb[TeSi(SiMe₃)₃]₂(TMEDA)₂ (2). The procedure used was analogous to that for the synthesis of **1**. The reaction of Yb[N(SiMe₃)₂]₂(THF)₂ (679 mg, 1.06 mmol) and HTeSi(SiMe₃)₃ (804 mg, 2.14 mmol) yielded orange plates of **2** (769 mg, 63%). Anal. Calcd for C₃₀H₈₆N₄Si₈Te₂Yb: C, 31.17; H, 7.50; N, 4.85. Found: C, 31.43; H, 6.91; N, 5.02. Mp: 176–177 °C dec. ¹H NMR: δ 2.44 (s, 24 H), 2.22 (s, 8 H), 0.46 (s, 54 H). ¹³C{¹H} NMR: δ 56.6, 50.0, 1.64. ¹²⁵Te{¹H} NMR: δ 610. IR (cm^{–1}): 1412 w, 1301 w, 1291 w, 1242 s, 1187 w, 1163 w, 1126 w, 1070 w, 1029 m, 1012 w, 954 m, 920 w, 837 s, 785 m, 742 w, 686 s, 622 s.

Eu[SeSi(SiMe₃)₃]₂(TMEDA)₂ (3). The procedure used was analogous to that for the synthesis of **1**. The reaction of Eu[N(SiMe₃)₂]₂(THF)₂ (281 mg, 0.456 mmol) and HSeSi(SiMe₃)₃ (300 mg, 0.915 mmol) yielded thin yellow needles of **3** (473 mg, 72%). Anal. Calcd for C₃₀H₈₆N₄Si₈Se₂Eu: C, 34.73; H, 8.35; N, 5.40. Found: C, 34.12; H, 8.14; N,

- (36) Wachter, P. In *Handbook of the Physics and Chemistry of Rare Earths*; Gschneidner, K. A., Eyring, L., Eds.; North-Holland: Amsterdam, 1979; Vol. 2, Chapter 19.
 (37) Tilley, T. D.; Andersen, R. A.; Zalkin, A. *J. Am. Chem. Soc.* **1982**, *104*, 3725.
 (38) Steigerwald, M. L.; Sprinkle, C. R. *J. Am. Chem. Soc.* **1987**, *109*, 7200.
 (39) Arnold, J.; Walker, J. M.; Yu, K. M.; Bonasia, P. J.; Seligson, A. L.; Bourret, E. D. *J. Cryst. Growth* **1992**, *124*, 647.
 (40) Stuczynski, S. M.; Brennan, J. G.; Steigerwald, M. L. *Inorg. Chem.* **1989**, *28*, 4431.
 (41) Brennan, J. G.; Siegrist, T.; Carroll, P. J.; Stuczynski, S. M.; Reynders, P.; Brus, L. E.; Steigerwald, M. L. *Chem. Mater.* **1990**, *2*, 403.

- (42) Tilley, T. D.; Zalkin, A.; Andersen, R. A.; Templeton, D. H. *Inorg. Chem.* **1981**, *20*, 551.
 (43) Rad'kov, Y. F.; Fedorova, E. A.; Khorshev, S. Y.; Kalinina, G. S.; Bochkarev, M. N.; Razuvaev, G. A. *Russ. J. Gen. Chem. (Engl. Transl.)* **1985**, *55*, 1911.
 (44) Evans, W. J.; Drummond, D. K.; Zhang, H.; Atwood, J. L. *Inorg. Chem.* **1988**, *27*, 575.
 (45) Watson, P. L.; Tulip, T. H.; Williams, I. *Organometallics* **1990**, *9*, 1999.
 (46) The synthesis of KSeSi(SiMe₃)₃ was analogous to that of KTeSi(SiMe₃)₃.¹⁷
 (47) Burt, R. J.; Chatt, J.; Hussain, W.; Leigh, G. J. *J. Organomet. Chem.* **1979**, *182*, 203.
 (48) Evans, D. F.; James, T. A. *J. Chem. Soc., Dalton Trans* **1979**, 723.
 (49) Selwood, P. W. *Magnetochemistry*, 2nd ed.; Interscience: New York, 1956.

5.05. Mp 202–207 °C dec. $\mu = 8.1 \mu_B$. IR (cm⁻¹): 1358 w, 1299 w, 1291 m, 1236 s, 1183 w, 1161 m, 1129 m, 1100 w, 1073 m, 1031 s, 1017 m, 953 s, 922 w, 864 s, 839 s, 783 s, 741 m, 685 s, 623 s.

EuTeSi(SiMe₃)₃h(TMEDA)₂ (4). The procedure used was analogous to that for the synthesis of 1. The reaction of Eu[N(SiMe₃)₂]₂(THF)₂ (267 mg, 0.433 mmol) and HTeSi(SiMe₃)₃ (326 mg, 0.887 mmol) yielded thin yellow plates of 4 (269 mg, 55%). Anal. Calcd for C₃₀H₈₆N₄Si₈Te₂Eu: C, 31.75; H, 7.64; N, 4.94. Found: C, 31.71; H, 7.72; N, 4.64. Mp: 84–88 °C dec. $\mu = 8.0 \mu_B$. IR (cm⁻¹): 1302 w, 1292 w, 1236 s, 1185 w, 1163 w, 1129 w, 1072 w, 1031 m, 1015 w, 954 m, 863 s, 836 s, 783 m, 742 w, 687 m, 622 m.

Sm[SeSi(SiMe₃)₃h(TMEDA)₂ (5). **Method A.** A solution of KSeSi(SiMe₃)₃ (799 mg, 2.18 mmol) in 30 mL of diethyl ether was added to a suspension of SmI₂(THF)₂ (597 mg, 1.09 mmol) in 30 mL of diethyl ether and 5 mL of TMEDA, resulting in the immediate formation of a dark green solution with a light blue precipitate. After 15 min of stirring, the volatiles were removed under vacuum. Extraction of the resulting solid with 200 mL of hexanes, followed by concentration and cooling to -40 °C, yielded thin dark green needles of 5 (490 mg, 43%). Repeated recrystallizations from hexanes and other solvents failed to remove minor -SiMe₃-containing decomposition products, preventing analytically pure material from being isolated. Mp: 191–192 °C dec. $\mu = 3.4 \mu_B$. ¹H NMR: δ 5.96 (s, 24 H, $\Delta\nu_{1/2} = 44$ Hz), 1.30 (s, 54 H, $\Delta\nu_{1/2} = 4.5$ Hz), -20.05 (s, 8 H, $\Delta\nu_{1/2} = 19$ Hz). ¹³C{¹H} NMR: δ 0.89. IR (cm⁻¹): 2803 m, 1291 m, 1236 s, 1161 w, 1129 w, 1073 w, 1031 m, 1017 w, 952 m, 866 s, 836 s, 782 m, 741 w, 685 s, 623 s.

Method B. The procedure used was analogous to that for the synthesis of 1. The reaction of Sm[N(SiMe₃)₂]₂(THF)₂ (307 mg, 0.499 mmol) and HSeSi(SiMe₃)₃ (327 mg, 0.998 mmol) yielded very dark green needles of 5 (286 mg, 55%).

SmTeSi(SiMe₃)₃h(TMEDA)₂ (6). **Method A.** The procedure used was analogous to method A used for the synthesis of 5. The reaction of SmI₂(THF)₂ (498 mg, 0.908 mmol) and KTeSi(SiMe₃)₃ (754 mg, 1.82 mmol) yielded dark green plates of 6 (415 mg, 40%). As noted in the Discussion, analytically pure material could not be obtained, even after repeated recrystallization from hexanes. Mp: 157–158 °C dec. $\mu = 3.3 \mu_B$. ¹H NMR: δ 3.02 (s, 24 H, $\Delta\nu_{1/2} = 62$ Hz), 1.97 (s, 54 H, $\Delta\nu_{1/2} = 14$ Hz), -21.02 (s, 8 H, $\Delta\nu_{1/2} = 93$ Hz). ¹³C{¹H} NMR: δ 1.59. ¹²⁵Te-¹H NMR: δ 3243. IR (cm⁻¹): 2797 m, 1301 w, 1292 m, 1237 s, 1185 w, 1162 w, 1129 w, 1071 w, 1031 m, 1015 m, 953 m, 862 s, 835 s, 783 m, 742 w, 686 s, 622 s.

Method B. The procedure used was analogous to that for the synthesis of 1. The reaction of Sm[N(SiMe₃)₂]₂(THF)₂ (254 mg, 0.413 mmol) and HTeSi(SiMe₃)₃ (310 mg, 0.824 mmol) yielded thin dark green plates of 6 (245 mg, 53%).

[Eu[SeSi(SiMe₃)₃h(DMPE)₂]₂(μ -DMPE) (7). The addition of 30 mL of diethyl ether to a flask containing Eu[N(SiMe₃)₂]₂(THF)₂ (601 mg, 0.974 mmol) and HSeSi(SiMe₃)₃ (714 mg, 2.18 mmol) resulted in the immediate formation of a homogeneous yellow solution. The addition of DMPE (0.82 mL, 4.9 mmol) resulted in the solution immediately turning orange. After 15 min of stirring, the volatiles were removed under vacuum. Extraction of the resulting solid with 100 mL of hexanes, followed by concentration and cooling to -40 °C, yielded thin orange needles of 7 (793 mg, 69%). Mp: 170–171 °C dec. $\mu = 8.0 \mu_B$. Anal. Calcd for C₆₆H₁₈₈P₁₀Si₁₆Se₄Eu₂: C, 33.57; H, 8.03. Found: C, 33.20; H, 8.08. IR (cm⁻¹): 1423 m, 1296 w, 1280 w, 1253 w, 1235 s, 1183 w, 1095 w, 945 m, 924 w, 903 w, 885 w, 864 m, 834 s, 724 m, 684 m, 622 m.

[EuTeSi(SiMe₃)₃h(DMPE)₂]₂(μ -DMPE) (8). **Method A.** A solution of HTeSi(SiMe₃)₃ (552 mg, 1.47 mmol) in 10 mL of hexanes was added over a 10-min period to a solution of Eu[N(SiMe₃)₂]₃ (596 mg, 0.941 mmol) and DMPE (0.25 mL, 1.5 mmol) in 30 mL of hexanes. Over the course of a few minutes, the solution turned dark green and an orange precipitate formed. The mixture was stirred for 1 h and the volatiles removed under vacuum. All of the material was extracted with 50 mL of hexanes, and concentration and cooling to -40 °C yielded small orange blocks of 8 in two crops (363 mg, 58%). Recrystallization from hexanes gave crystals suitable for X-ray diffraction. Mp: 182–183 °C dec. $\mu = 8.0 \mu_B$. Anal. Calcd for C₆₆H₁₈₈P₁₀Si₁₆Te₄Eu₂: C, 31.02; H, 7.41. Found: C, 30.52; H, 7.46. IR (cm⁻¹): 1424 m, 1297 w, 1236 m, 1182 w, 1095 w, 946 m, 923 w, 904 w, 890 w, 863 m, 835 s, 723 w, 686 w, 623 w.

Method B. The procedure used was analogous to that for the synthesis of 7. The reaction of Eu[N(SiMe₃)₂]₂(THF)₂ (302 mg, 0.489 mmol), HTeSi(SiMe₃)₃ (361 mg, 0.982 mmol), and DMPE (0.40 mL, 2.4 mmol) yielded small orange blocks of 8 (312 mg, 50%).

Solid-State Thermolyses of 1 and 2. Approximately 200 mg (0.2 mmol) of the compound was placed in a quartz boat inside a long quartz tube. The tube was placed under a dynamic vacuum of 10⁻² Torr and heated in a tube furnace to 300 °C over the course of about 2 h. At a temperature of about 150–200 °C, a colorless (E = Se) or yellow (E = Te) wax condensed in the unheated end of the tube. Over the same temperature range, the color of the solid in the boat turned black. The temperature of the tube was held at 300 °C for about 3 h. For annealing purposes, the temperature was increased to 800 °C and maintained there for 12 h.

After the tube was slowly cooled to room temperature, the wax recovered was identified as pure E[Si(SiMe₃)₃]₂ by ¹H and ¹³C NMR comparisons to authentic samples (¹H NMR: E = Se, δ 0.35; E = Te, δ 0.36. ¹³C NMR: E = Se, δ 1.45; E = Te, δ 1.90). The black powder remaining in the boat was analyzed by CHN combustion analyses (typically: C, <3%, H and N, 0.0%) and X-ray powder diffraction. The yield of YbE was typically 100–110%, most likely due to Si and C impurities. Lit. [d (Å)]: YbSe,⁵⁰ 3.430 w, 2.967 s, 2.098 m, 1.789 w, 1.713 w, 1.484 w, 1.327 w, 1.211 w; YbTe,⁵¹ 3.184 s, 2.252 m, 1.836 w, 1.591 w, 1.424 w, 1.300 w, 1.125 w, 1.061 w. Found [d (Å)]: YbSe, 3.419 w, 2.967 s, 2.098 m, 1.794 w, 1.711 w, 1.485 w, 1.327 w, 1.207 w; YbTe, 3.174 s, 2.246 m, 1.835 w, 1.589 w, 1.422 w, 1.298 w, 1.124 w, 1.059 w.

X-ray Crystallography. Table 1 contains details of crystal and data collection parameters. The structure of 8 was determined by Dr. F. J. Hollander at the CHEXRAY crystallographic facility in the College of Chemistry, University of California, Berkeley, CA.

1. Small orange needles were obtained by slow crystallization from a saturated hexanes solution at -40 °C. A suitable fragment was cleaved and mounted on a glass fiber using Paratone N hydrocarbon oil. The crystal was transferred to an Enraf-Nonius CAD-4 diffractometer, centered in the beam, and cooled to -104 °C. Automatic peak search and indexing procedures yielded a monoclinic reduced primitive cell. Inspection of the systematic absences indicated the space group P2₁/c.

The 3848 raw intensity data were converted to structure factor amplitudes and their esd's by correction for scan speed, background, and Lorentz and polarization effects. Intensity standards were measured on the diffractometer every 1 h of data collection. Intensity standards decreased 2.8% over the data collection period. Three reflections were checked after every 250 measurements as orientation checks. Crystal orientation was redetermined if any of the reflections were offset by more than 0.01° from their predicted positions; such orientation was necessary eight times during data collection. Inspection of the azimuthal scan data showed a variation $I_{\min}/I_{\max} = 0.81$ for the average curve. An empirical correction based on the observed variation was applied to the data. Removal of systematic absences left 3408 unique reflections. Removal of 146 data that deviated more than 0.10° from their calculated positions left 3262 reflections.

The crystal structure was solved using Patterson methods and refined by standard least-squares and Fourier techniques. Following refinement of all non-hydrogen atoms with anisotropic thermal parameters, all hydrogen atoms were assigned idealized positions. They were included in the structure factor calculations, but not refined.

The final residuals for 205 variables against the 1986 data for which $F^2 > 3\sigma(F^2)$ were $R = 0.0437$, $R_w = 0.0424$, and GOF = 1.21. The R value for all 3262 data was 0.103. The largest peak in the final difference Fourier map had an electron density of 0.48 e/Å³, and the lowest excursion was -0.37 e/Å³.

8. Large orange blocks were obtained by slow crystallization from a saturated hexanes solution at -40 °C. A suitable fragment was cleaved and mounted on a glass fiber using Paratone N hydrocarbon oil. The crystal was transferred to an Enraf-Nonius CAD-4 diffractometer, centered in the beam, and cooled to -90 °C. Automatic peak search and indexing procedures yielded a triclinic reduced primitive cell. Inspection of the Niggli values revealed no conventional cell of higher symmetry.

The 11125 raw intensity data were converted to structure factor amplitudes and their esd's by correction for scan speed, background, and Lorentz and polarization effects. Intensity standards were measured on the diffractometer every 1 h of data collection and showed no significant decrease in intensity over the data collection period. Three reflections were checked after every 200 measurements as orientation checks. Crystal orientation was redetermined if any of the reflections were offset by more than 0.01° from their predicted positions; such orientation was necessary twice during data collection. Inspection of the azimuthal scan data showed

a variation $I_{\min}/I_{\max} = 0.86$ for the average curve. An empirical correction based on the observed variation was applied to the data. The choice of the centric space group $P\bar{1}$ was confirmed by the successful solution and refinement of the structure.

The crystal structure was solved using Patterson methods and refined by standard least-squares and Fourier techniques. The SiMe_3 groups attached to Te1 are disordered in two positions, one of which is occupied 13% of the time. Disorder was modeled by changing the occupancy until the effective isotropic thermal parameters for the two sets of partially occupied atoms were equal. The Si atoms were modeled, but no attempt was made to find the minority carbon atoms. Many of the carbon atoms are nearly in the same place for either Si configuration. In addition, a similar modeling technique indicated that the methyl carbon atoms on Si8 were disordered in two positions, in the ratio of about 45:55. In a difference Fourier map calculated following the refinement of all nondisordered non-hydrogen atoms with anisotropic thermal parameters, peaks were found corresponding to the positions of many of the hydrogen atoms. Hydrogen atoms for ordered carbon atoms were assigned idealized locations and values of B_{iso} were approximately 1.25 times the B_{eqv} of the atoms to which they were attached. They were included in the structure factor calculations, but not refined.

The final residuals for 452 variables against the 8565 data for which $F^2 > 3\sigma(F^2)$ were $R = 0.0350$, $R_w = 0.0410$, and $\text{GOF} = 1.52$. The R value for all 11125 data was 0.0524. In the final cycles of refinement a secondary extinction parameter was included (maximum correction was 10% on F). The largest peak in the final difference Fourier map had an electron density of $1.32 \text{ e}/\text{\AA}^3$, and the lowest excursion was $-0.11 \text{ e}/\text{\AA}^3$. The largest peaks were all located near the Eu atom or the disordered SiMe_3 .

Acknowledgment. We thank the National Science Foundation (CHE-9210406) for financial support, the Department of Education for a fellowship to D.R.C., the Alfred P. Sloan Foundation for the award of a research fellowship to J.A., Prof. A. M. Stacy for the use of XRD and SQUID equipment, and Dr. V. Christou for conducting preliminary studies in this work.

Supplementary Material Available: Tables of intramolecular distances and angles, least-squares planes, positional parameters, and temperature factor expressions (18 pages). Ordering information is given on any current masthead page.